

Lecture Notes in Civil Engineering

Gabriella Bolzon
Donatella Sterpi
Guido Mazzà
Antonella Frigerio *Editors*

Numerical Analysis of Dams

Proceedings of the 15th ICOLD
International Benchmark Workshop

 Springer

Lecture Notes in Civil Engineering

Volume 91

Series Editors

Marco di Prisco, Politecnico di Milano, Milano, Italy

Sheng-Hong Chen, School of Water Resources and Hydropower Engineering,
Wuhan University, Wuhan, China

Ioannis Vayas, Institute of Steel Structures, National Technical University of
Athens, Athens, Greece

Sanjay Kumar Shukla, School of Engineering, Edith Cowan University, Joondalup,
WA, Australia

Anuj Sharma, Iowa State University, Ames, IA, USA

Nagesh Kumar, Department of Civil Engineering, Indian Institute of Science
Bangalore, Bengaluru, Karnataka, India

Chien Ming Wang, School of Civil Engineering, The University of Queensland,
Brisbane, QLD, Australia

Lecture Notes in Civil Engineering (LNCE) publishes the latest developments in Civil Engineering—quickly, informally and in top quality. Though original research reported in proceedings and post-proceedings represents the core of LNCE, edited volumes of exceptionally high quality and interest may also be considered for publication. Volumes published in LNCE embrace all aspects and subfields of, as well as new challenges in, Civil Engineering. Topics in the series include:

- Construction and Structural Mechanics
- Building Materials
- Concrete, Steel and Timber Structures
- Geotechnical Engineering
- Earthquake Engineering
- Coastal Engineering
- Ocean and Offshore Engineering; Ships and Floating Structures
- Hydraulics, Hydrology and Water Resources Engineering
- Environmental Engineering and Sustainability
- Structural Health and Monitoring
- Surveying and Geographical Information Systems
- Indoor Environments
- Transportation and Traffic
- Risk Analysis
- Safety and Security

To submit a proposal or request further information, please contact the appropriate Springer Editor:

- Mr. Pierpaolo Riva at pierpaolo.riva@springer.com (Europe and Americas);
- Ms. Swati Meherishi at swati.meherishi@springer.com (Asia—except China, and Australia, New Zealand);
- Dr. Mengchu Huang at mengchu.huang@springer.com (China).

All books in the series now indexed by Scopus and EI Compendex database!

More information about this series at <http://www.springer.com/series/15087>

Gabriella Bolzon · Donatella Sterpi ·
Guido Mazzà · Antonella Frigerio
Editors

Numerical Analysis of Dams

Proceedings of the 15th ICOLD International
Benchmark Workshop

 Springer

Editors

Gabriella Bolzon
Department of Civil and Environmental
Engineering (DICA)
Politecnico di Milano
Milano, Italy

Donatella Sterpi
Department of Civil and Environmental
Engineering (DICA)
Politecnico di Milano
Milano, Italy

Guido Mazzà
Italian Committee on Large Dams
(ITCOLD)
Roma, Italy

Antonella Frigerio
Ricerca sul Sistema Energetico—RSE SpA
Milano, Italy

ISSN 2366-2557

ISSN 2366-2565 (electronic)

Lecture Notes in Civil Engineering

ISBN 978-3-030-51084-8

ISBN 978-3-030-51085-5 (eBook)

<https://doi.org/10.1007/978-3-030-51085-5>

© The Editor(s) (if applicable) and The Author(s), under exclusive license to Springer Nature Switzerland AG 2021

This work is subject to copyright. All rights are solely and exclusively licensed by the Publisher, whether the whole or part of the material is concerned, specifically the rights of translation, reprinting, reuse of illustrations, recitation, broadcasting, reproduction on microfilms or in any other physical way, and transmission or information storage and retrieval, electronic adaptation, computer software, or by similar or dissimilar methodology now known or hereafter developed.

The use of general descriptive names, registered names, trademarks, service marks, etc. in this publication does not imply, even in the absence of a specific statement, that such names are exempt from the relevant protective laws and regulations and therefore free for general use.

The publisher, the authors and the editors are safe to assume that the advice and information in this book are believed to be true and accurate at the date of publication. Neither the publisher nor the authors or the editors give a warranty, expressed or implied, with respect to the material contained herein or for any errors or omissions that may have been made. The publisher remains neutral with regard to jurisdictional claims in published maps and institutional affiliations.

This Springer imprint is published by the registered company Springer Nature Switzerland AG
The registered company address is: Gewerbestrasse 11, 6330 Cham, Switzerland

Seismic Behavior of a Bituminous-Faced Rock-Fill Dam: The Menta Dam



L. Petkovski, S. Mitovski, and F. Panovska

Abstract In the analysis of the dynamic response of the bituminous-faced rock-fill dam (BFRD) Menta, is applied non-linear model, where the rock material is approximated by variable sliding modulus, and the asphaltic facing with thickness of 32 cm is applied by joint elements with linear elastic constitutive law. Permanent displacements during the seismic excitation are determined by Dynamic deformation analysis, where the incremental forces are calculated by the difference of the effective stresses in two successive time steps, resulting in adequate deformations. For the state of reservoir rapid filling, as pre-earthquake state by normal water elevation in the reservoir, is used elastoplastic model by variable modulus of elasticity for the rock material. By the dynamic analysis is verified the seismic resistance of the fill dam at action of design earthquakes by PGA of 0.26 g, without disruption of the water impermeability of the asphaltic facing and without danger for rapid and uncontrolled emptying of the reservoir, because the settlements in the dam crest caused by dynamic inertial forces for the earthquake duration amounts 40 cm, i.e. they are much lower than the height above normal elevation in the reservoir till the dam crest, with value of 7.25 m.

Keywords Menta dam · Dynamic analysis · Asphaltic facing

1 Dam Model and Material Parameters for the Structural Analysis

The representative cross section and parameters of the local materials for the fill dam Menta are adopted according to the available data bases [1]. The model for structural (static and dynamic) analysis of the dam is composed of two materials: rock material in the dam's body and asphaltic facing (Fig. 1). For the static analysis,

L. Petkovski (✉) · S. Mitovski · F. Panovska
Civil Engineering Faculty, University Ss. Cyril and Methodius, Skopje, North Macedonia
e-mail: petkovski@gf.ukim.edu.mk

Macedonian Committee on Large Dams, Skopje, North Macedonia

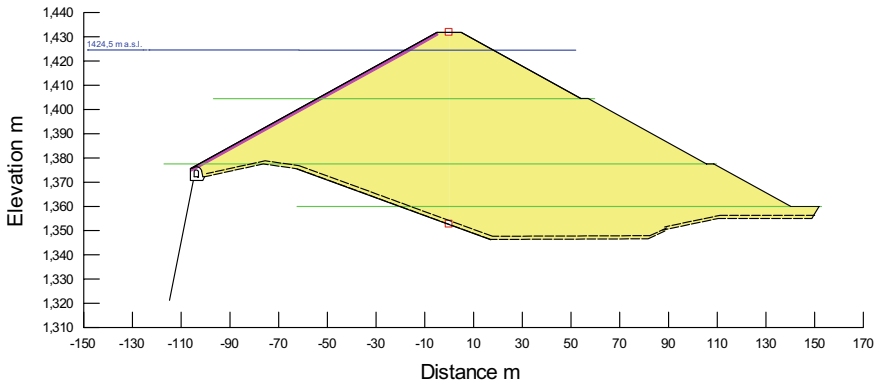


Fig. 1 Model for structural analysis, by specified elevations: dam crest at 1,431.75 m asl, normal water elevation at 1,424.5 m asl, first berm on 1,404.5 m asl, second berm on 1,377.5 m asl, upstream toe at 1,375.53 m asl (above grouting gallery), rock at cross section axis 1,352.57 m asl, downstream toe at 1,360.0 m asl. Structural height of 1,431.75–1,352.57 = 79.18 m

for the asphaltic facing, with thickness of 0.32 m is applied linear elastic law, by following material parameters: $E = 150,000 \text{ kPa}$, $\nu = 0.44$, $\gamma = 24 \text{ kN/m}^3$, while for the rock material is applied elastoplastic constitutive law with variable modulus of elasticity (Fig. 2), with following geo-mechanical parameters: $E = E(\sigma_y')$, $\nu = 0.27$, $\gamma = 23 \text{ kN/m}^3$, $\phi = 38^\circ$ and $c = 0.0 \text{ kN/m}^2$.

For the dynamic analysis, for the asphalt facing with thickness of 0.32 m is applied linear elastic law, by following material parameters: $G_{\max} = 2.0 \text{ GPa}$, $\nu = 0.44$, $\gamma = 24 \text{ kN/m}^3$, $DR = 0.1$, while for the rock material is applied non-linear constitutive

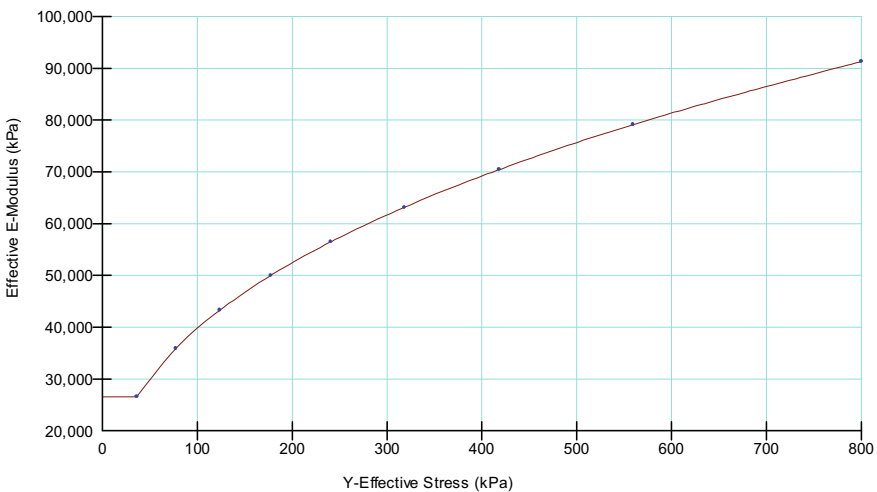


Fig. 2 Variable static modulus of elasticity for rock material $E = E(\sigma_y')$

law with variable maximal sliding modulus (Fig. 3), by following geo-mechanical parameters: $G_{max} = G(\sigma_y')$, $\nu = 0.27$, $\gamma = 23 \text{ kN/m}^3$, $DR = 0.05\text{--}0.25$, $\varphi = 38^\circ$ and $c = 0.0 \text{ kN/m}^2$. The applied dependence $G_{max} = G(\sigma_y')$ is adopted by using of variation of small-strain Young modulus (E_0) with confining pressure (σ'_3), obtained in cyclic triaxial tests, (from Table 1, page 10). Available results from laboratory tests: physical and mechanical properties of rock-fill material (Fig. 4) and using of expressions: $k_0 = 1 - \sin\varphi$, where $\varphi = 38^\circ$, $\nu = k_0 / (1 + k_0)$, $G_{max} = E_{dyn} / [2(1 + \nu)]$, $\sigma'_y = \sigma'_x / k_0$.

The plane model for dam Menta is discretized with finite element mesh, Fig. 5.

For determination of the internal static values (bending moments M , axial forces N and transversal forces Q) in the asphaltic facing, it has been replaced with structural

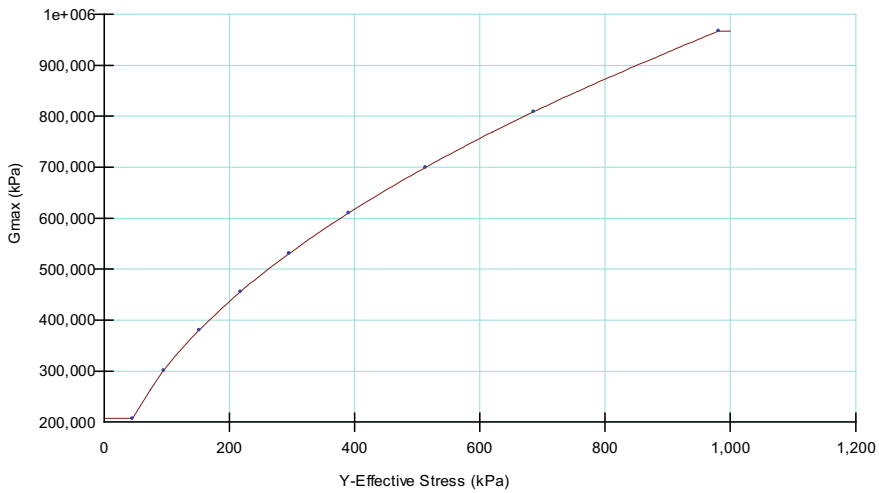


Fig. 3 Variable maximal sliding modulus for rock material $G_{max} = G(\sigma_y')$

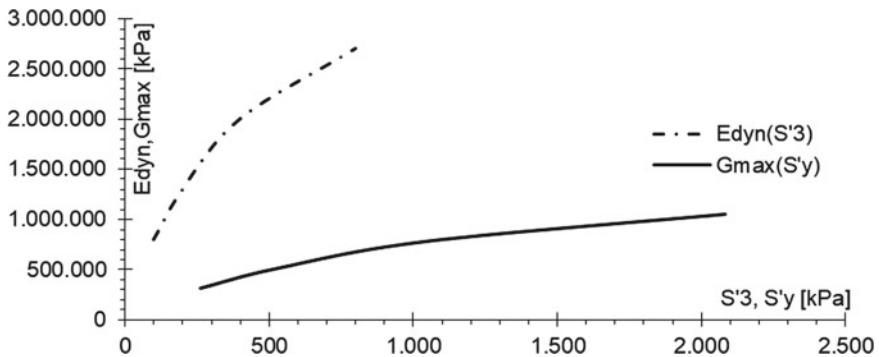


Fig. 4 Dynamic material parameters for the rock material, $E_{dyn}(\sigma'_3)$ —given (from Table 1, page 10) and $G_{max}(\sigma'_y)$ —estimated

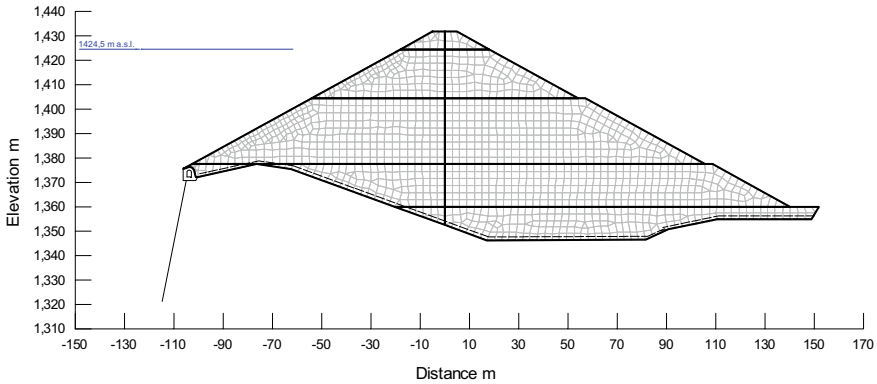


Fig. 5 Discretization of the medium with finite element mesh, nodes $N = 1,444$, elements $E = 1,373$, by application of non-linear model and joint elements for the asphaltic facing with $d = 0.32$ m

element with: moment of inertia $I = 1.0 \cdot 0.323 / 12 = 0.002731 \text{ m}^4$, cross section $F = 1.0 \cdot 0.32 = 0.32 \text{ m}^2$ and modulus of elasticity $E = 150,000 \text{ kPa}$. The model for structural analysis of the dam is discretized with finite element mesh, Fig. 6, where as the dynamic analysis is conveyed by equivalent linear analysis (ELA) with the following non-elastic dynamic parameters for the rock material, Figs. 7 and 8.

The applied approach in the present analysis for determination of the permanent deformations during the seismic excitation, for any node within the fill dam, is the method of “Dynamic Deformation Analysis” (DDA), which is successive non-linear redistribution of the stresses [2]. By such method, for geo-medium discretized by finite elements, are calculated deformations caused by forces in nodes, calculated by the incremental stresses in the elements. Thus, by application of non-linear model,

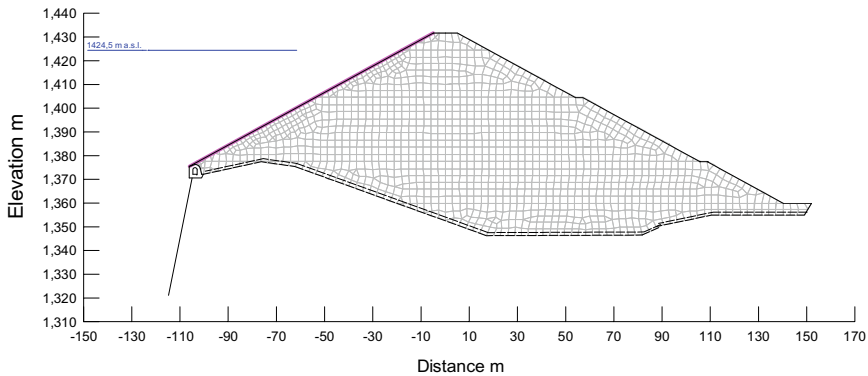


Fig. 6 Discretization of the medium with finite element mesh, nodes $N = 1,384$, elements $E = 1,313$, by application of equivalent linear law with structural element for the asphaltic facing with $h = 0.32$ m

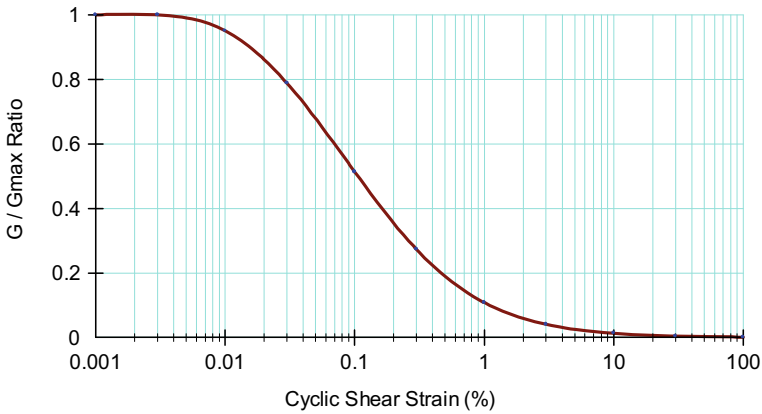


Fig. 7 Reduction of the sliding modulus by rise of the tangential strains for the rock material by application of equivalent linear analysis

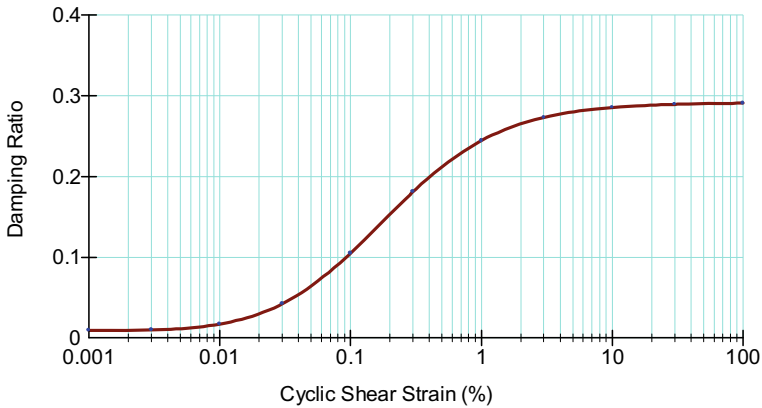


Fig. 8 Rise of the damping coefficient by rise of the tangential strains for the rock material by application of equivalent linear law

for each time step of the dynamic response of the structure [3] is obtained new state of the total stresses and pore pressure.

By the differences of the effective stresses in two successive time steps are obtained incremental forces, resulting in deformations, in accordance with the chosen constitutive law for dependence stress—strain. So, for each loading case during the dam’s dynamic response are produced elastic and eventual plastic strains. If dynamic inertial forces cause plastic strains, then in the geo-medium will occur permanent deformations. The permanent displacements, at any point in the dam and at end of the seismic excitation, are cumulative sum of the plastic deformations.

2 State at Full Reservoir

The initial state for first filling of the reservoir is the state after construction of the dam, Figs. 9 and 10. The stress state after dam construction and state at first filling of the reservoir is obtained using the program Sigma/W [2].

The state at first filling of the reservoir is modeled in 10 increments, by linear rise of the water level in the reservoir from the upstream toe at elevation 1,375.53 m asl, till elevation of normal water level at 1,424.5 m asl, apropos for water head of $1,424.5 - 1,375.53 = 48.97$ m. For such stress state are displayed stresses (Figs. 11 and 12), distribution of the modulus of elasticity, Fig. 13, as well and incremental displacements (Figs. 14 and 15).

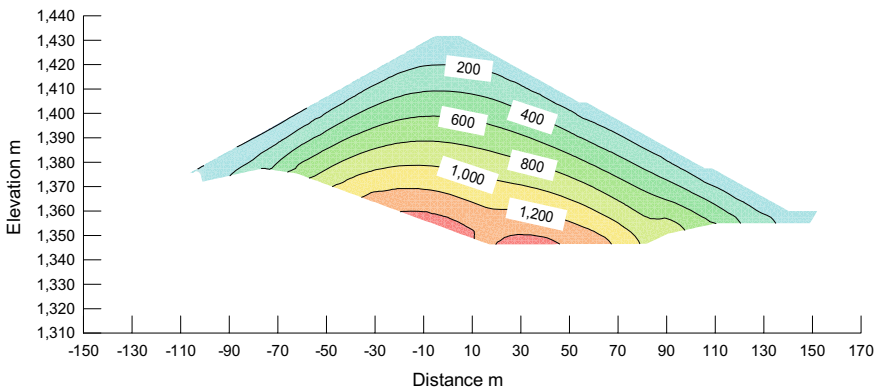


Fig. 9 Distribution of vertical effective stresses after dam construction, $\sigma'_y = 1,461.3$ kPa

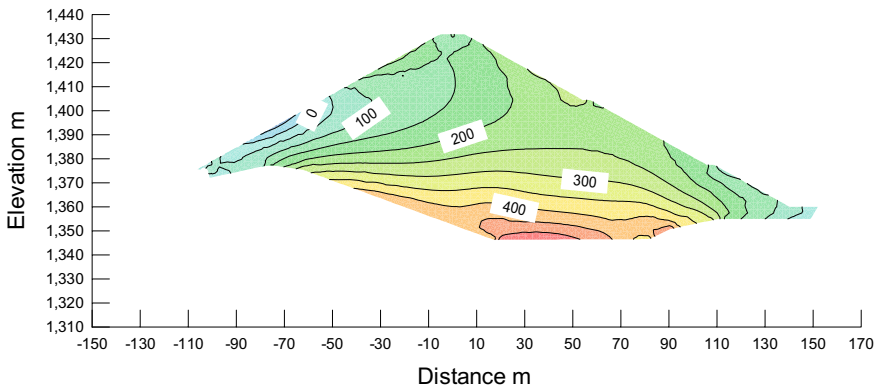


Fig. 10 Distribution of horizontal effective stresses after dam construction, $\sigma'_{x, \max} = 540.78$ kPa

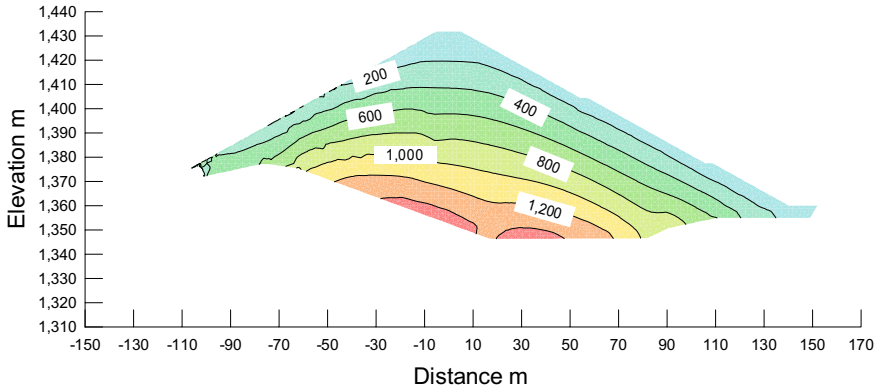


Fig. 11 Distribution of vertical effective stresses after reservoir filling, $\sigma'_{y, \max} = 1,492$ kPa

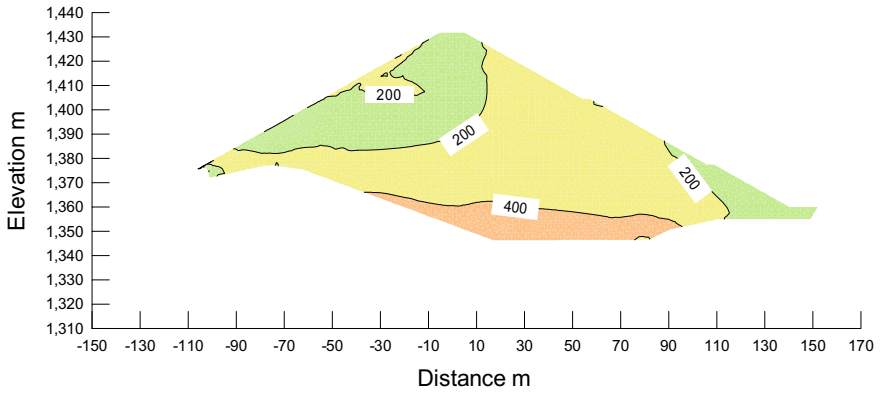


Fig. 12 Distribution of horizontal effective stresses after reservoir filling, $\sigma'_{x, \max} = 700.0$ kPa

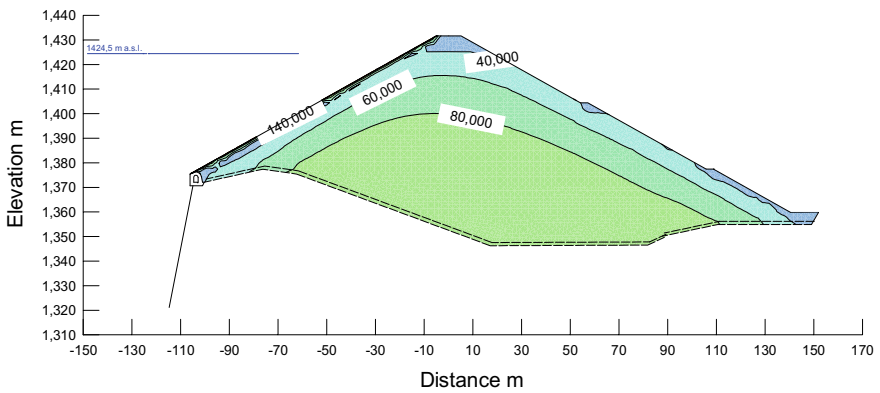


Fig. 13 Distribution of modulus of elasticity after reservoir filling, $E_{\max} = 150,000.0$ kPa

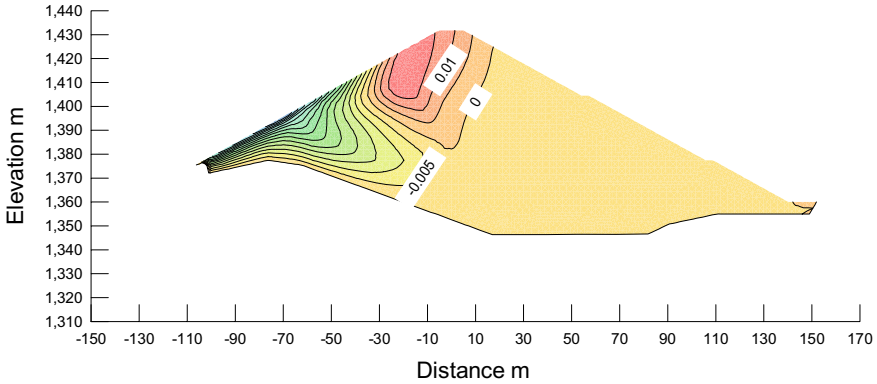


Fig. 14 Distribution of incremental vertical displacements after reservoir filling, $dY = 0.074 + 0.019 \text{ m}$

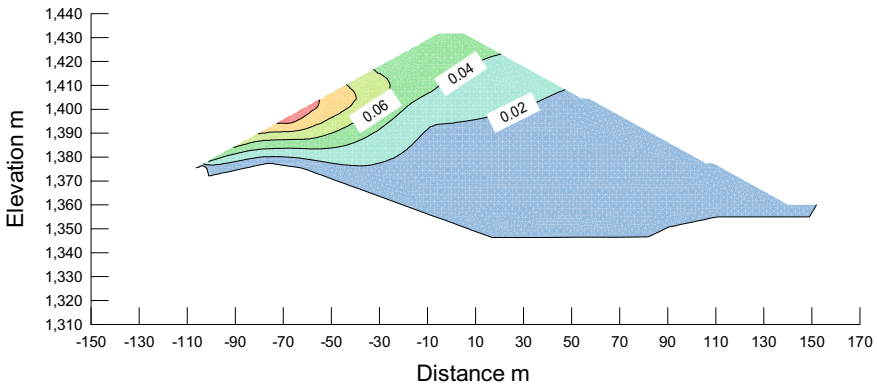


Fig. 15 Distribution of incremental horizontal displacements after reservoir filling, $dX = 0.000, +0.110 \text{ m}$

3 Fundamental (Eigen) Periods of the Dam

For determination of the fundamental periods for certain level of non-elastic response of the fill dam is used dynamic excitation of synthetic harmony vibration by continuous change of the frequencies apropos by evenly represented frequencies in the interval $f1 \div f2 = 0.4 \div 10.0 \text{ [Hz]}$ or periods $T1 \div T2 = 2.5 \div 0.1 \text{ [s]}$. Such harmonium is with: two values of the maximal amplitude $Ao = 0.05, 0.30 \text{ g}$, summary duration $St = 12 \text{ s}$, by the time increment in the accelegram $dt = 0.01 \text{ s}$, Fig. 16. Response spectrum of the excitation and response, spectral acceleration $Sa \text{ [g]}$ for damping coefficient $DR = 0.05$, are displayed in Figs. 17 and 18 (for empty reservoir) and Figs. 19 and 20 (for full reservoir). The dynamic response of the dam is determined by use of the program Quake/W [3].

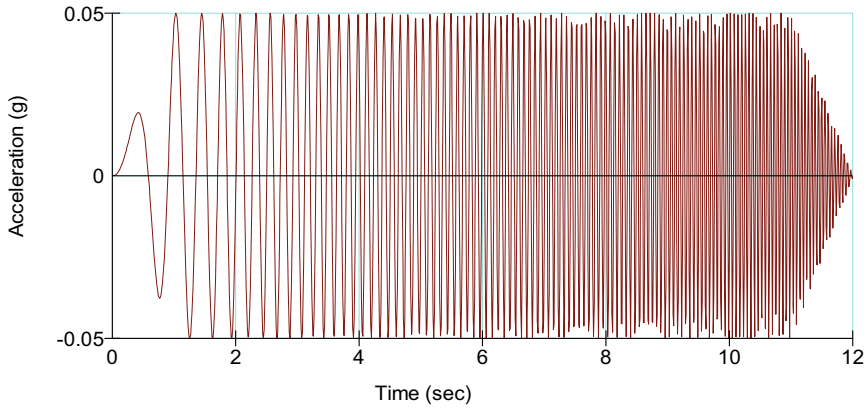


Fig. 16 Time history of horizontal displacements of harmonic vibration by evenly represented frequencies $f_1 \div f_2 = 0.4 \div 10.0$ [Hz], scaled by $A_o = 0.05$ g

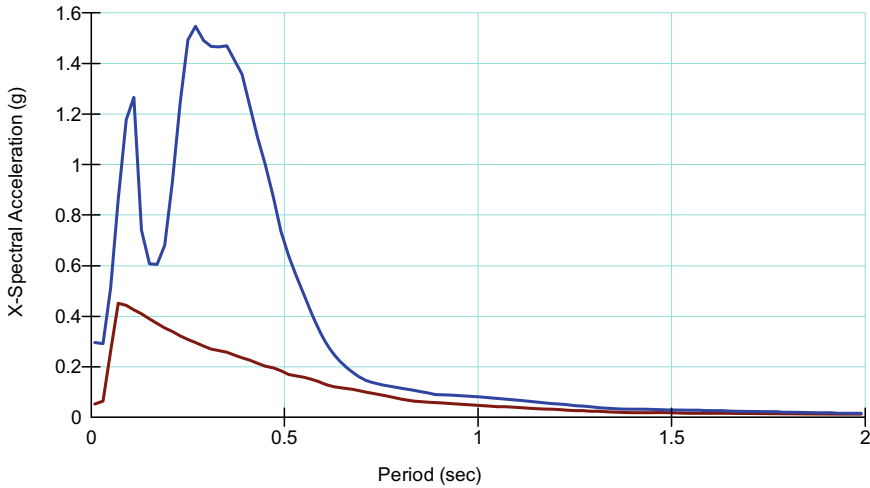


Fig. 17 Response spectrum of absolute accelerations in the dam crest at empty reservoir, caused by harmonic oscillation with low intensity $PGA = 0.05$ g, with first Eigen period $T_1 = 0.32$ s

4 Response at Action of Friuli Earthquake 1976

The accelerogram of the horizontal and vertical component of the Friuli earthquake 1976 are displayed on Figs. 21 and 22.

Horizontal displacements in the dam crest at action of such earthquake are displayed on Fig. 23, and the response spectra of the accelerations are displayed on Fig. 24.

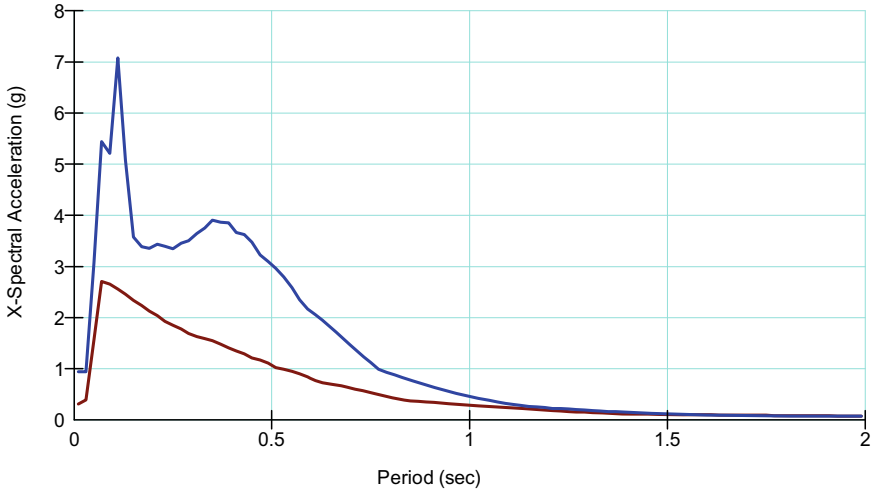


Fig. 18 Response spectrum of absolute accelerations in the dam crest at empty reservoir, caused by harmonic oscillation with high intensity $PGA = 0.30$ g, with first Eigen period $T1 = 0.39$ s

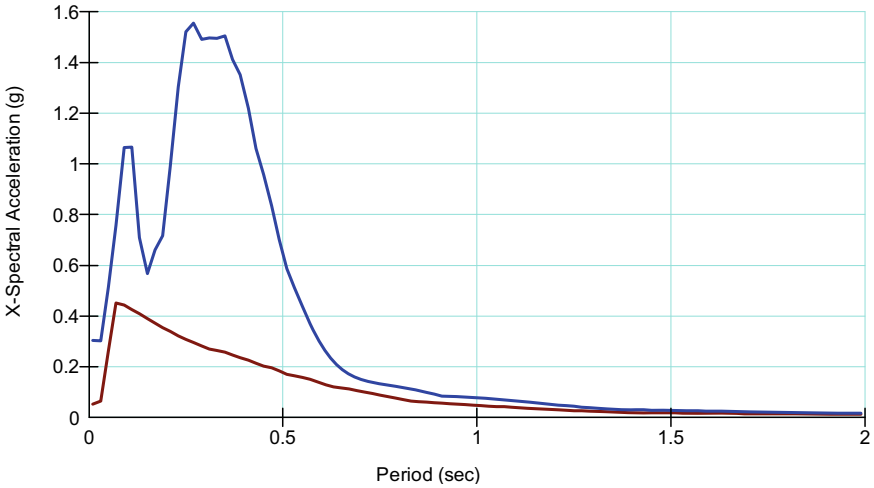


Fig. 19 Response spectrum of absolute accelerations in the dam crest at full reservoir, caused by harmonic oscillation with low intensity $PGA = 0.05$ g, with first Eigen period $T1 = 0.31$ s

Relative displacements at the dam crest at action of such earthquake are displayed on Fig. 25.

Permanent horizontal and vertical displacements at the dam crest during action of such earthquake are displayed on Figs. 26 and 27.

Permanent horizontal and vertical displacements at the dam axis after action of such earthquake are displayed on Figs. 28 and 29. Maximal shear and volumetric

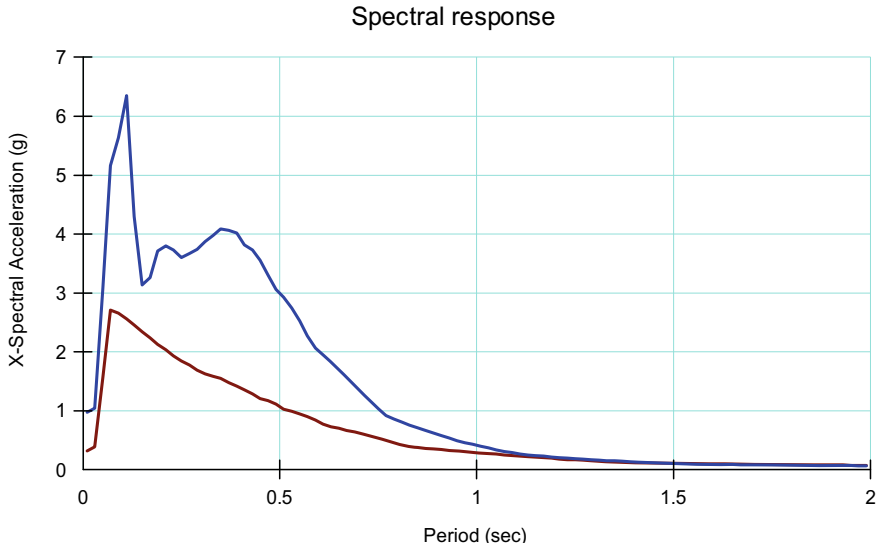


Fig. 20 Response spectrum of absolute accelerations in the dam crest at full reservoir, caused by harmonic oscillation with low intensity $PGA = 0.30\text{ g}$, with first Eigen period $T1 = 0.37\text{ s}$

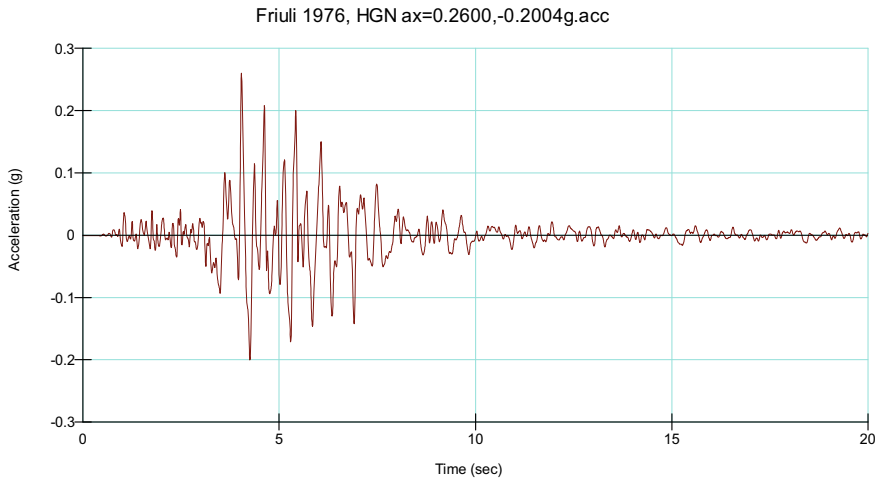


Fig. 21 Time history of horizontal component of the excitation in the rock foundation for Friuli earthquake 1976, $PGA = 0.26\text{ g}$

strains in the upstream slope of the dam, at asphaltic facing during the earthquake are displayed on Figs. 30 and 31.

Permanent displacements in XY direction in the dam after action of such earthquake are displayed in Fig. 32.

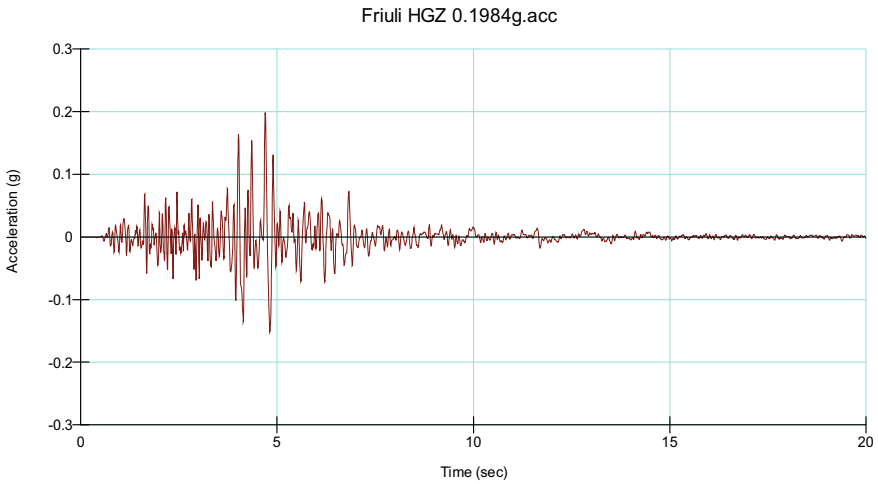


Fig. 22 Time history of vertical component of the excitation in the rock foundation for Friuli earthquake 1976

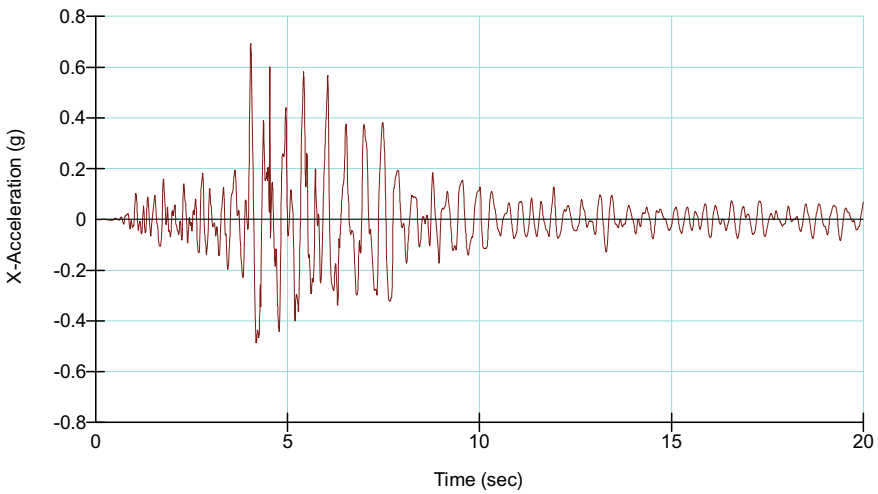


Fig. 23 Time history of horizontal component of the response at dam crest at action of Friuli earthquake 1976, PCE = 0.693 g

By application of equivalent linear model are obtained similar relative displacements at dam crest (compared to nonlinear model), Fig. 33, and the value of the axial forces in the asphaltic facing is displayed on Fig. 34.

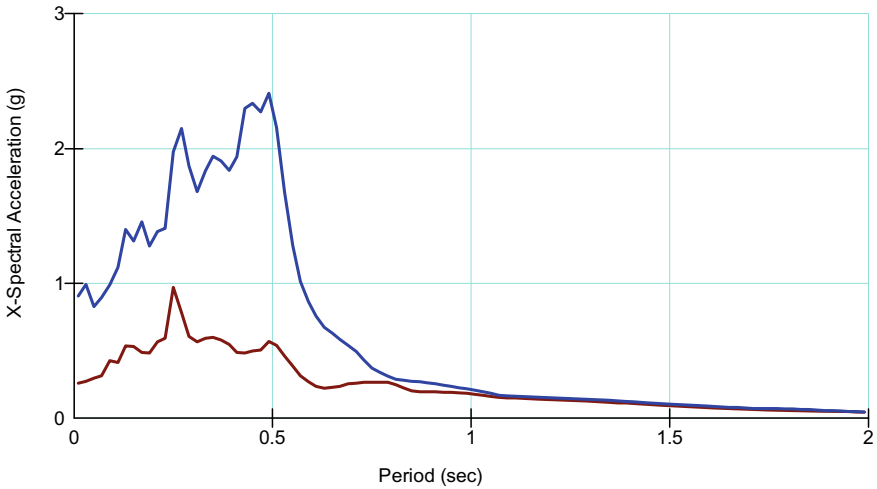


Fig. 24 Response spectra for accelerations in the foundation and at the dam crest at action of Friuli earthquake 1976

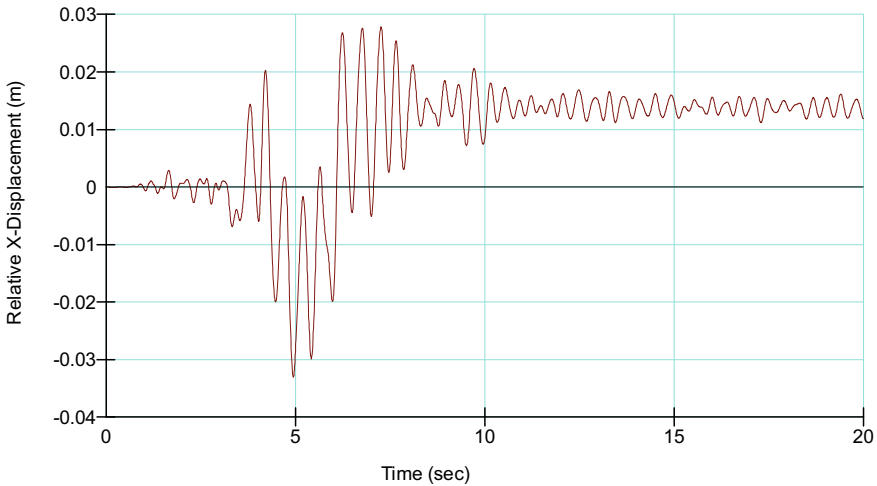


Fig. 25 Relative horizontal displacements at dam crest at action of Friuli earthquake 1976

5 Response at Action of Central Italy Earthquake 2016

Accelerograms of the horizontal and vertical component of Central Italy earthquake 2016 are displayed on Figs. 35 and 36.

Horizontal accelerations in the dam crest at action of such earthquake are displayed on Fig. 37, and the response spectra of the accelerations are displayed on Fig. 38.

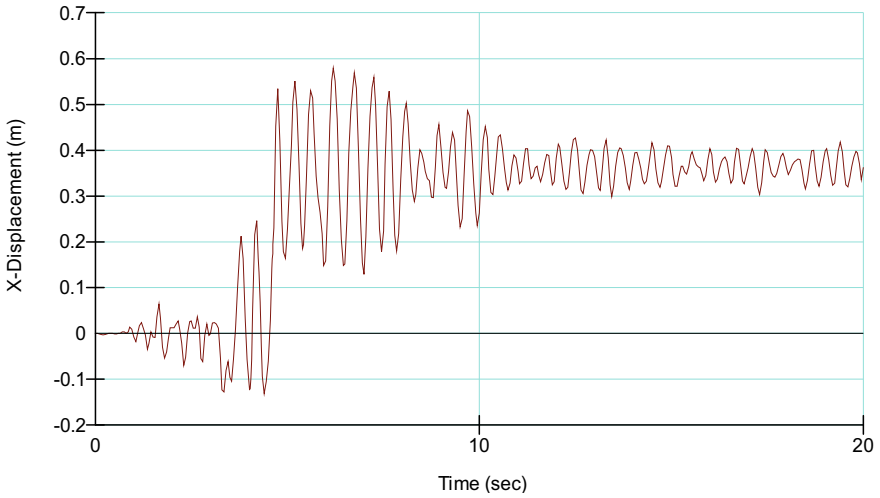


Fig. 26 Permanent horizontal displacements at dam crest at action of Friuli earthquake 1976

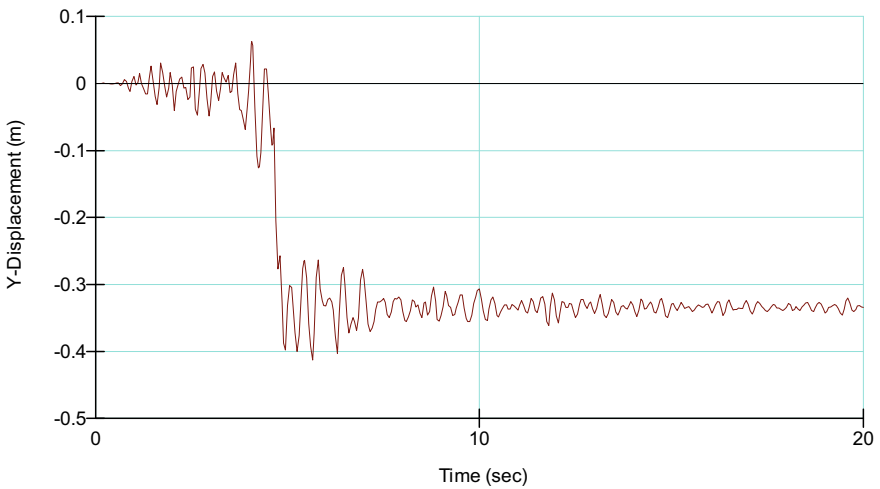


Fig. 27 Permanent vertical displacements at dam crest at action of Friuli earthquake 1976

Relative displacements at dam crest at action of such earthquake are displayed on Fig. 39.

Permanent horizontal and vertical displacements at dam crest at action of such earthquake are displayed on Figs. 40 and 41.

Permanent horizontal and vertical displacements at dam crest after action of such earthquake are displayed on Figs. 42 and 43. Maximal shear and volumetric strains in

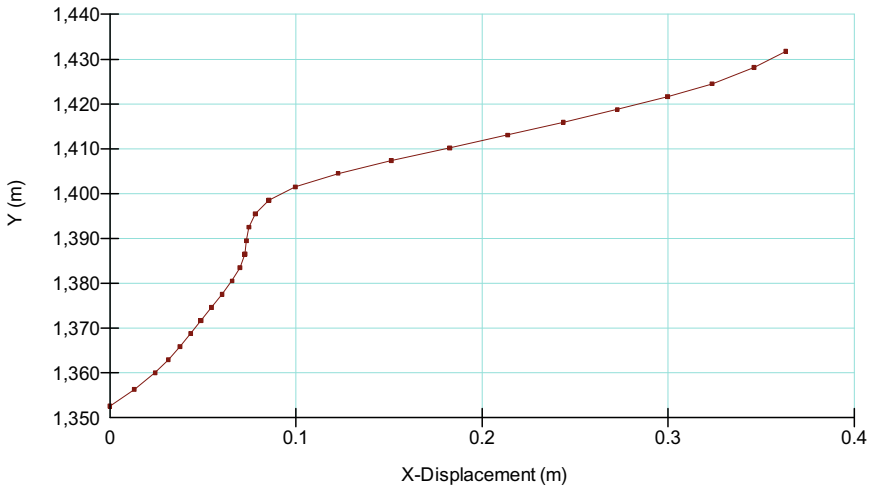


Fig. 28 Permanent horizontal displacements at dam crest axis after action of Friuli earthquake 1976, X = 0.363 m (downstream)

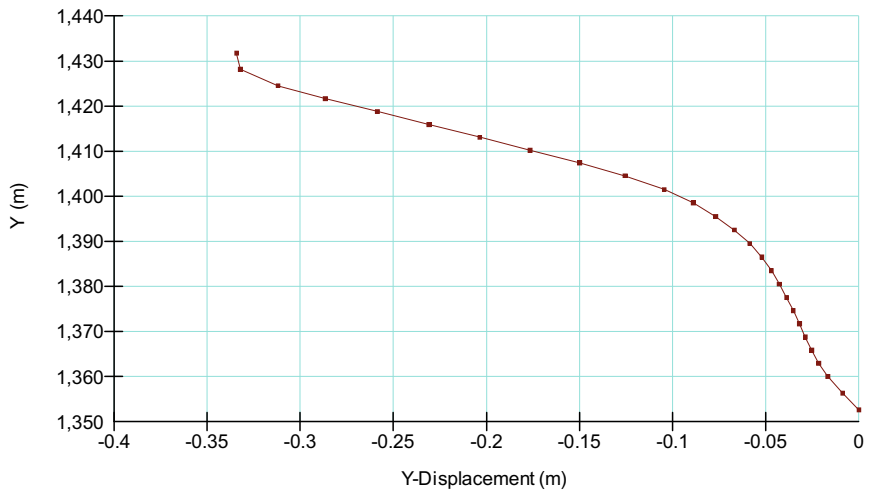


Fig. 29 Permanent vertical displacements at dam crest axis after action of Friuli earthquake 1976, Y = -0.334 m (settlement)

upstream slope of the dam, at asphaltic facing during such earthquake are displayed on Figs. 44 and 45.

Permanent displacements in XY direction after action of such earthquake are displayed on Fig. 46.

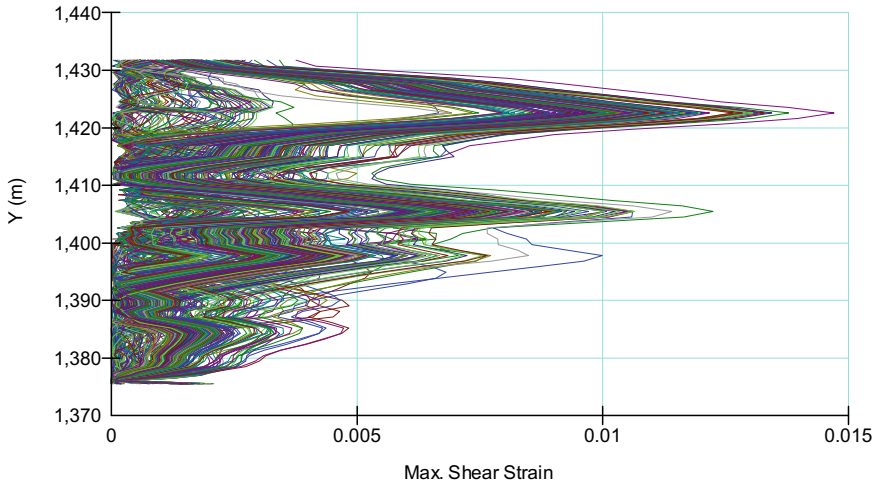


Fig. 30 Maximal shear strains in upstream slope of the dam, at asphaltic facing during Friuli earthquake 1976

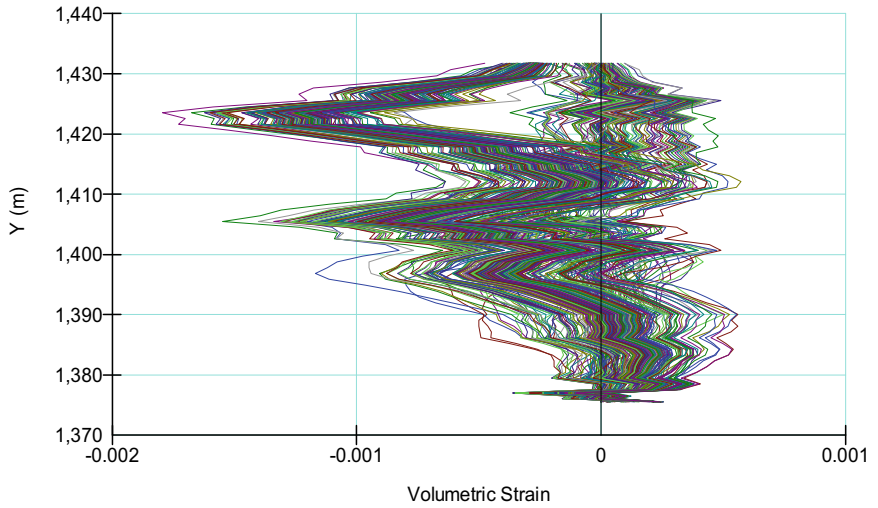


Fig. 31 Volumetric strains in upstream slope of the dam during Friuli earthquake 1976

By application of equivalent linear model (ELM) are obtained similar relative displacements at dam crest (compared with nonlinear model NLM), Fig. 47, and the value of the axial forces in the asphaltic facing is displayed on Fig. 48.

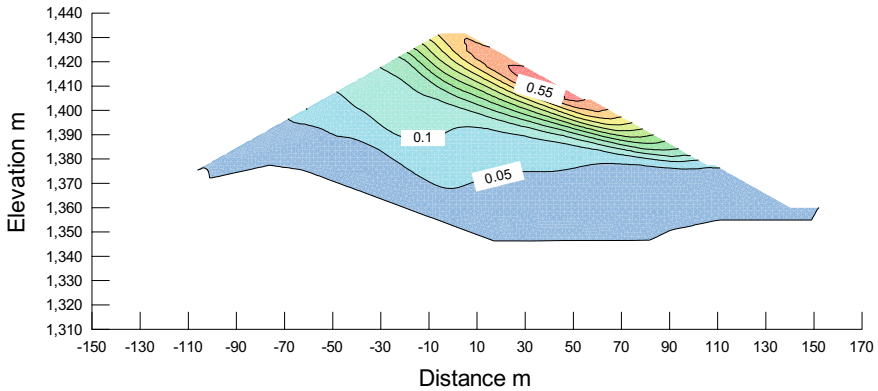


Fig. 32 Permanent displacements in XY direction in the dam after action of Friuli earthquake 1976, $XY_{max} = 0.580$ m

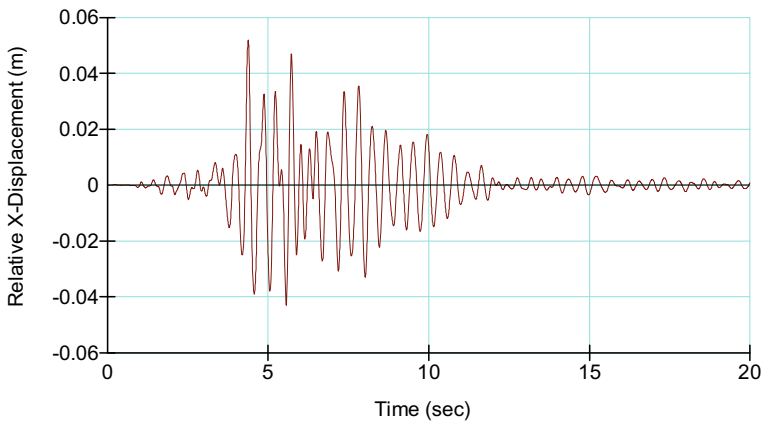


Fig. 33 Relative horizontal displacements at the dam crest at action of Friuli earthquake 1976, by application of equivalent linear model (ELM)

6 Conclusions

Eigen periods of the dam are determined by the response spectrum excited by harmonic vibration, by evenly represented frequencies of 0.4 to 10.0 Hz, scaled by PGA of 0.05 g (low excitement—L) to 0.30 g (high excitement—H). For low excitement (L), for initial state of stress at empty reservoir (E), first Eigen period is $T1LE = 0.32$ s, and for high excitement (H), is obtained $T1HE = 0.39$ s. In case of higher excitement, the response of the fill dam is more nonlinear, the stiffness of the rock material is decreased by increased non-elastic deformations, thus conditioning

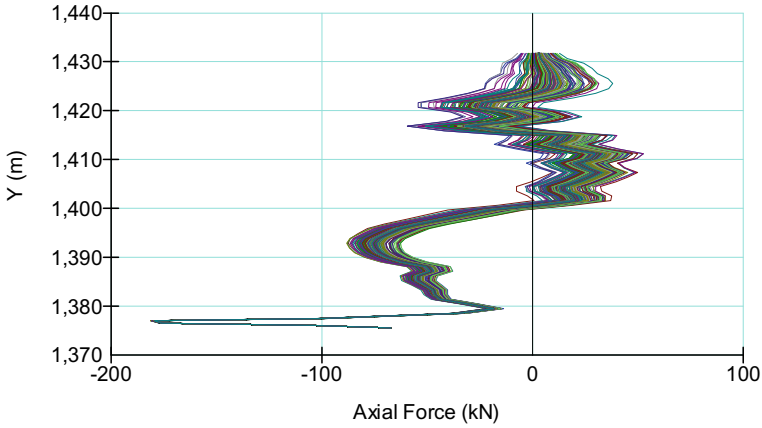


Fig. 34 Axial forces in the asphaltic facing at action of Friuli earthquake 1976, by application of equivalent linear model (ELM), $N = -181.3, 52.6$ kN

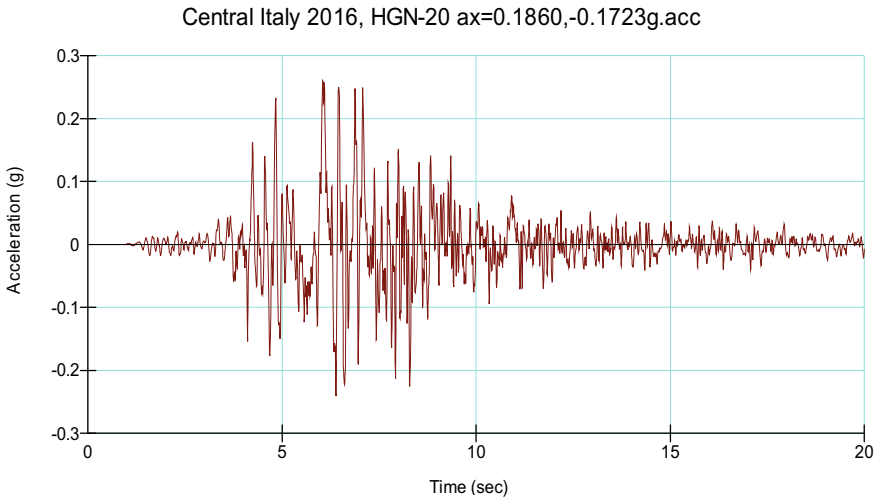


Fig. 35 Time history of horizontal component of the excitation in the rock foundation for Central Italy earthquake 2016, scaled on 0.26 g

rise of the period of the basic tone [4]. For initial stress state at full reservoir (F), below the hydrostatic pressure of the asphaltic facing the normal stresses are increased in the upstream part of the dam. As result of the increased stiffness of the rock material, for such state are obtained lower values for the basic tone (T1), apropos $T1LF = 0.31$ s and $T1HF = 0.37$ s. The values for the basic tone (T1), determined in the analysis, matches with the measured value for dams exposed on strong earthquakes

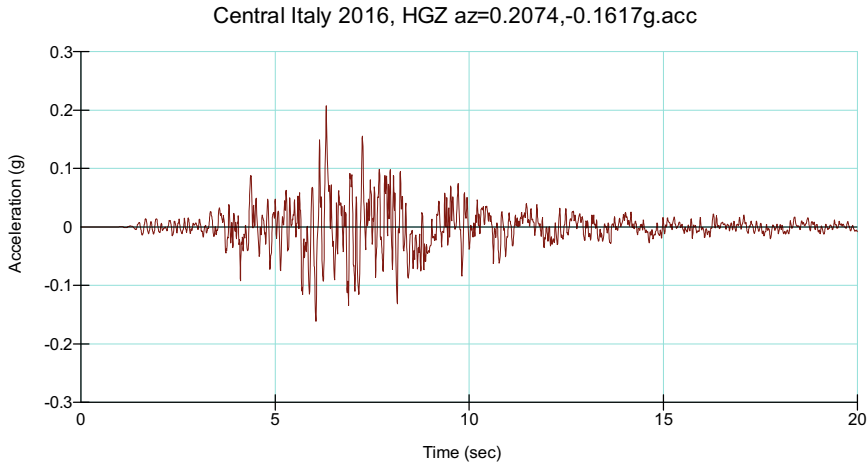


Fig. 36 Time history of vertical component of the excitation in the rock foundation for Central Italy earthquake 2016, scaled on 0.26 g

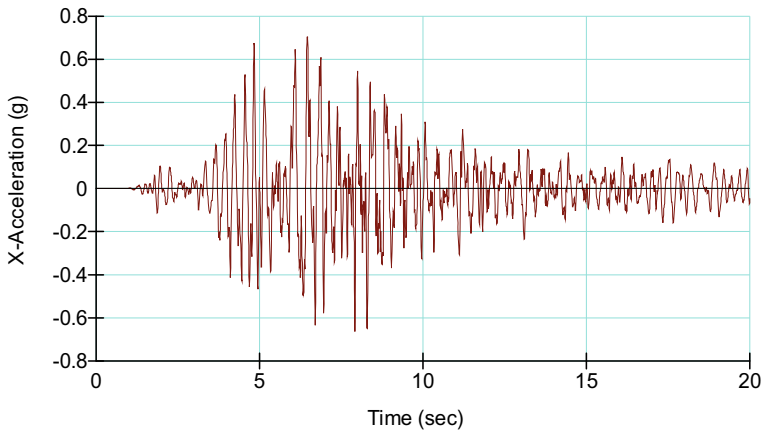


Fig. 37 Time history of the horizontal component of response at dam crest at action of Central Italy earthquake 2016, PCE = 0.698 g

in Japan [5, 6], that is best verification for the properly adopted dynamic material parameters for nonlinear dynamic analysis.

The values for Dynamic Amplification Factor $DAF = PCA/PGA$, where PGA is Peak Ground Acceleration (in horizontal direction), and PCA is Peak Crest Acceleration (in horizontal direction) are: $0.693/0.26 = 2.67$ in case of Friuli earthquake 1976 and $0.698/0.26 = 2.68$ in case of Central Italy earthquake 2016. The response at dam crest matches the registered data for the degree of dynamic amplification for

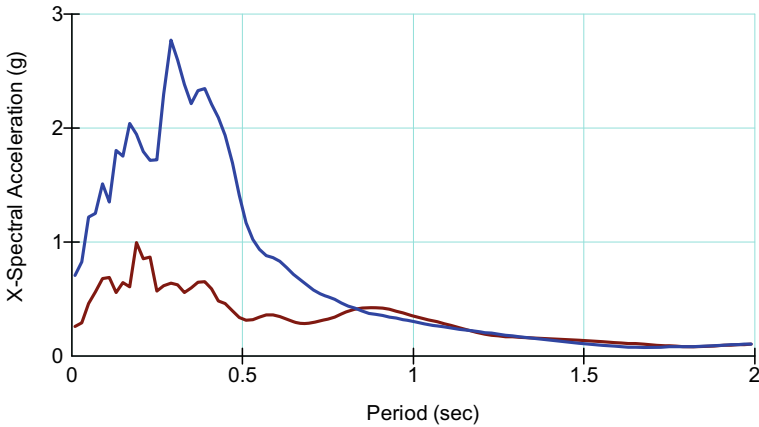


Fig. 38 Response spectra of the accelerations in the foundation and at dam crest at action of Central Italy earthquake 2016

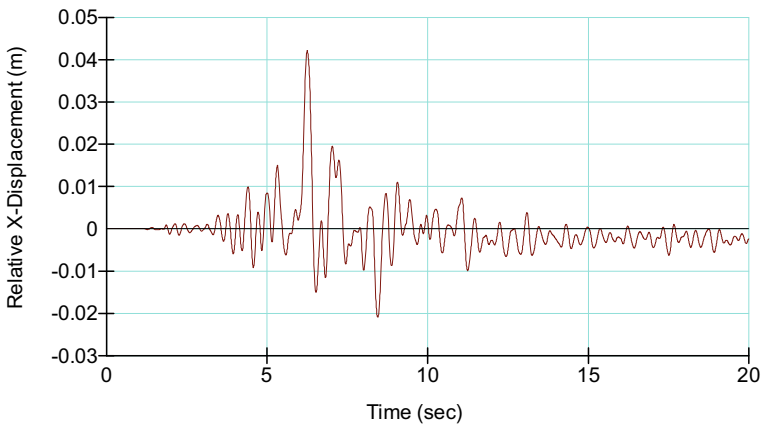


Fig. 39 Relative horizontal displacements at dam crest at action of Central Italy earthquake 2016

such structures under action of strong earthquakes, [7], apropos is the key indicator for the correctness of the dynamic analysis.

The permanent settlements at dam crest, caused by dynamic inertial forces for the duration of the earthquake, determined by the method of Dynamic Deformation Analysis, are $Y = -0.334$ m in case of Friuli earthquake 1976, and $Y = -0.399$ m in case of Central Italy earthquake 2016. Independently that in the analysis are not taken into account the settlements from additional compaction and decreased stiffness at materials exposed on cyclic action, the total settlement can not overcome the height

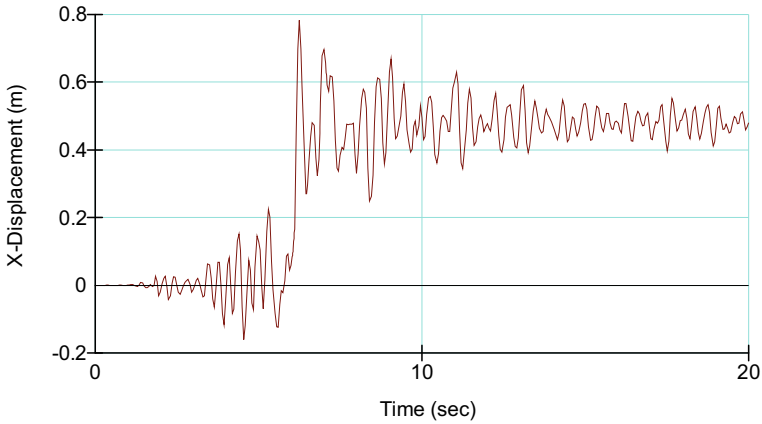


Fig. 40 Permanent horizontal displacements at dam crest at action of Central Italy earthquake 2016, $X = 0.480$ m

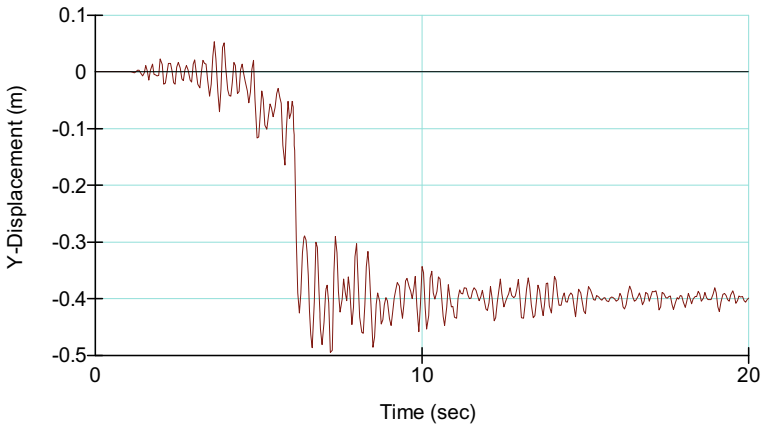


Fig. 41 Permanent vertical displacements at dam crest at action of Central Italy earthquake 2016, $Y = -0.399$ m

from dam crest (1431.75 m asl) till normal water elevation in the reservoir (1424.5 m asl), apropos height of 7.25 m.

The increase in permeability only occurred as fissures opened for shear deformations close to the failure level (strength) for the asphaltic facing. No significant increase was detectable until about 80% of the strength was mobilized [8]. Under moderate earthquake loading with $PGA = 0.26$ g, using the Friuli earthquake 1976 and Central Italy earthquake 2016, the induced deformations in dam body are small (XY_{max} ranges from 58.0 cm to 67.4 cm in the downstream slope of the dam), and

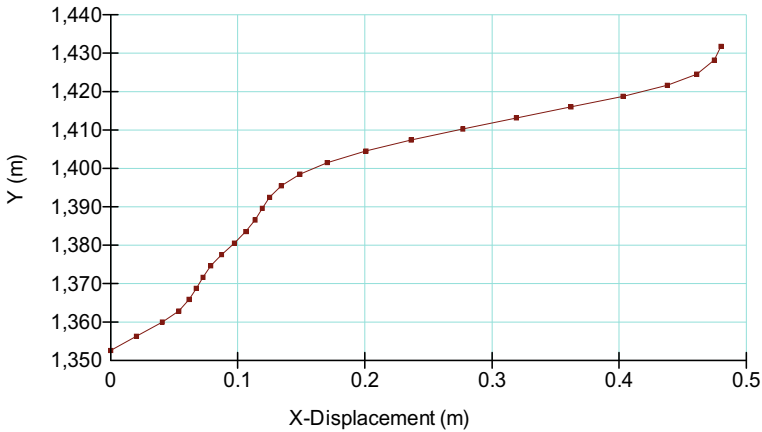


Fig. 42 Permanent horizontal displacements at dam crest axis after action of Central Italy earthquake 2016, at crest X = 0.480 m

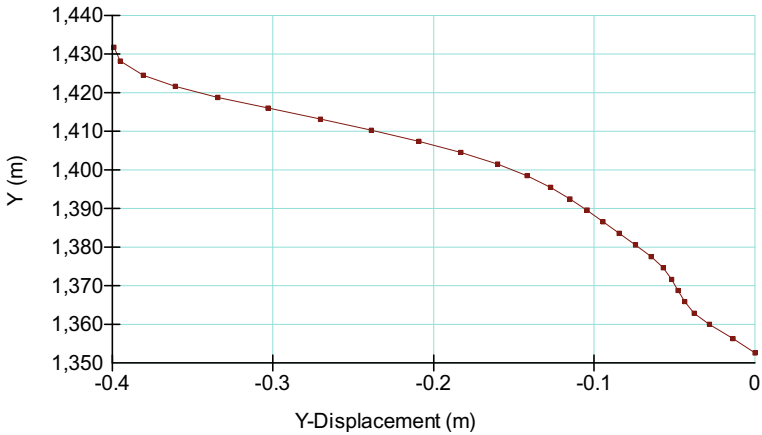


Fig. 43 Permanent vertical displacements at dam crest axis after action of Central Italy earthquake 2016, at crest Y = -0.399 m

the maximum shear strains in the asphalt facing are less than 1.5% and 1.8%, respectively. In these ranges of deformations, according to the results of permeability tests, the asphalt facing remains watertight. Therefore, it is expected that no damage will occur at Menta dam during the seismic excitation. At the same time, by application of equivalent linear analysis the asphaltic facing with thickness of 0.32 m is approximated by structural element and axial forces during the seismic excitation are calculated. By the dynamic response for both earthquakes is obtained maximal tension force of 181.3 kN (182.6 kN) and compression force of 52.6 kN (67.3 kN),

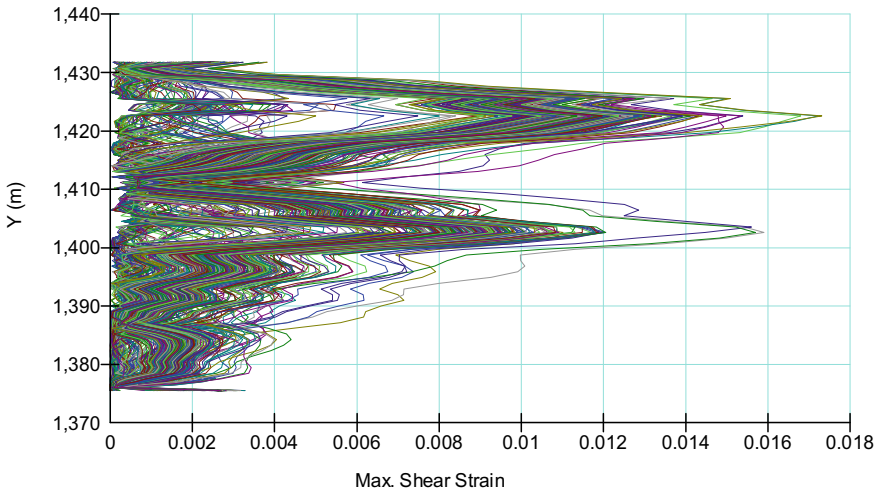


Fig. 44 Maximal shear strains in upstream slope of the dam at asphaltic facing during Central Italy earthquake 2016

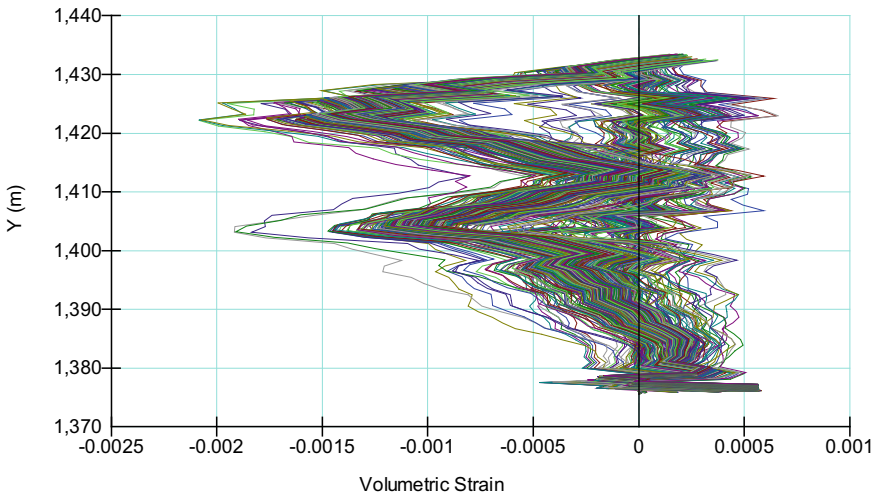


Fig. 45 Volumetric strains in upstream slope of the dam at asphaltic facing during Central Italy earthquake 2016

thus obtaining stresses much lower than the specific strength of the asphalt, such as compression strength of $f_c = 1.46$ GPa and tension strength of $f_t = 0.95$ GPa.

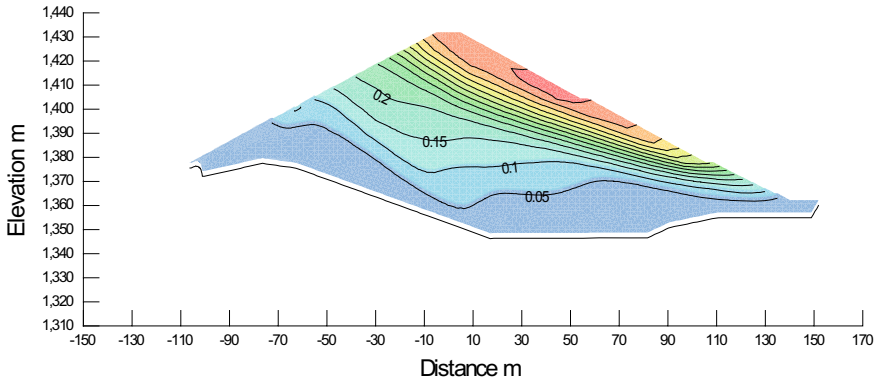


Fig. 46 Permanent displacements in XY direction in the dam after action of Central Italy earthquake 2016, $XY_{max} = 0.674$ m

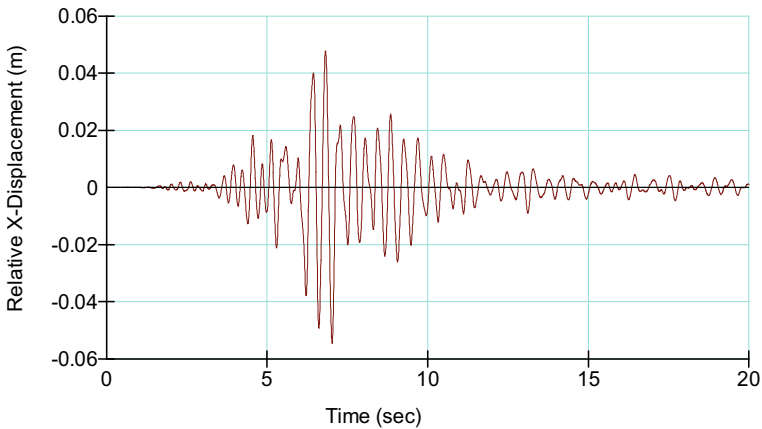


Fig. 47 Relative horizontal displacements at the dam crest at action of Central Italy earthquake 2016, by application of equivalent linear model (ELM)

The key conclusion from the dynamic analysis of rock-fill dam Menta with asphaltic facing is that the dam, by adopted geometry and material distribution, possesses satisfactory seismic resistance. There is no case of disruption of the water impermeability of the watertight element (asphaltic facing with thickness of 0.32 m), nor there is danger of rapid and uncontrolled emptying of the artificial lake, because by the calculated settlements for design earthquakes with PGA of 0.26 g the protection height of 7.25 m is not exceeded.

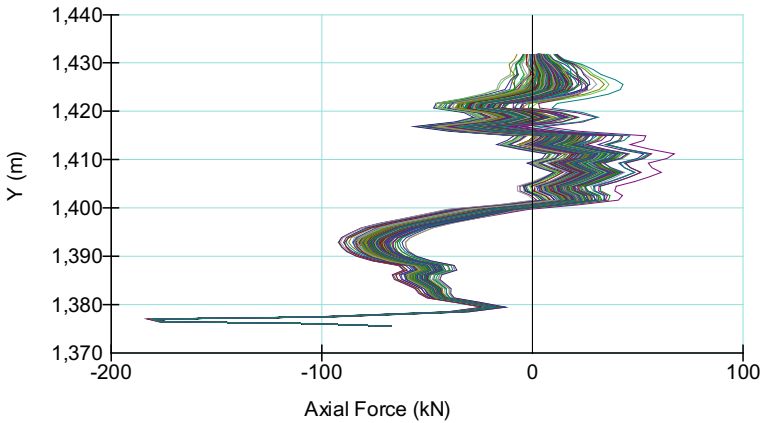


Fig. 48 Axial forces in the asphaltic facing at action of Central Italy earthquake 2016, by application of equivalent linear model (ELM), $N = -182.6, 67.3$ kN

References

1. Russo G, Vecchietti A, Cecconi M, Pane V, De Marco S, Florino A (2019) 15th international benchmark workshop on numerical analysis of dams, Theme B
2. Geo-Slope: SIGMA/W v8 (2017) User's Guide for finite element stress/deformation analysis. GEO-SLOPE International Ltd., Calgary, Alberta, Canada
3. Geo-Slope: QUAKE/W v8 (2017) Dynamic Modeling. GEO-SLOPE International Ltd., Calgary, Alberta, Canada
4. Park DS (2018) Fundamental period of embankment dams based on strong motion records, topic earthquakes—embankments. In: USSD 38th annual meeting and conference, a balancing act: dams, levees and ecosystems, April 3- May 4, 2018, Miami, Florida, USA, CD Proceedings
5. Matsumoto N, Ohmachi T, Yasuda N, Yamaguchi Y, Sasaki T, Kurahashi H (2005) Analysis of strong motions recorded at dams during earthquakes. In: 73rd annual meeting of ICOLD, Tehran, IRAN, Paper No.: 094-W
6. Fry JJ, Matsumoto N (2018) Validation of dynamic analyses of dams and their equipment, CRC Press/Balkema. Tailor & Francis Group, London, New York
7. ICOLD, Bulletin 113. Seismic observation of dams—Guidelines and case studies (1999)
8. Hoeg K (1993) Asphaltic Concrete cores for embankment dams—experience and practice. Norwegian Geotechnical Institute of Technology, Oslo, Norway